J|A|C|S
ARTICLES
Published on Web 09/06/2003

Photochemistry of Ortho, Ortho′ Dialkyl Phenyl Azides

Meng-Lin Tsao and Matthew S. Platz*

Contribution from the Department of Chemistry, The Ohio State University, 100 West 18th Avenue, Columbus, Ohio 43210

Received April 28, 2003; E-mail: platz.1@osu.edu

Abstract: Phenyl azide, 2,6-diethylphenyl azide, 2,6-diisopropylphenyl azide, and 2,4,6-tri-*tert*-butylphenyl azide were studied by laser flash photolysis (LFP) methods. LFP (266 nm) of the azides in glassy 3-methylpentane at 77 K produces the transient UV−vis absorption spectra of the corresponding singlet nitrenes. At 77 K, the singlet nitrenes relax to the corresponding triplet nitrenes. The triplet nitrenes are persistent at 77 K and their spectra were recorded. The rate constants of singlet to triplet intersystem crossing were determined at this temperature. LFP of 2,4,6-tri-*tert*-butyl phenyl azide in pentane at ambient temperature again produces a singlet nitrene, which is too short-lived to detect by nanosecond spectroscopy under these conditions. Unlike the other azides, the first detectable intermediate produced upon LFP of 2,4,6-tri-*tert*-butyl phenyl azide at ambient temperature is the benzazirine (285 nm) which has a lifetime of 62 ns controlled by ring opening to a didehydroazepine. The results are interpreted with the aid of Density Functional Theoretical and Molecular Orbital Calculations.

I. Introduction

The chemistry of aryl azides has a long history that dates back to the 19th century and has been reviewed several times.[1−3] Phenyl azide was first synthesized by Greiss in 1864.[4] Since then, many derivatives have been the subject of extensive investigation because of their important biological and industrial applications as photoaffinity labeling agents,[5,6] cross-linking reagents in photoresists,[7] the formation of conducting polymers,[8] and the light induced activation of polymer surfaces.[9,10]

The mechanistic details of the decomposition of phenyl azide are complex,[11] and have been studied extensively by analysis of reaction mixtures, matrix-isolation spectroscopy, laser flash photolysis (LFP), and modern molecular orbital (MO) theory. Several reactive intermediates are formed on photolysis of phenyl azide, the key intermediate among them is the singlet phenylnitrene **1a** (Scheme 1).

The existence of singlet phenylnitrene **1a** was demonstrated in 1997 by its direct detection upon laser flash photolysis (LFP) of phenyl azide **2a**.[12−14] The transient spectrum of **1a** displays a sharp and intense band at 350 nm. Kinetic studies of this transient provide information about the lifetime of **1a** at ambient temperature (∼1 ns), the barrier to its rearrangement (5.6 kcal/mol), and the rate constant of intersystem crossing (ISC, 3×10^6 s^{-1}) of singlet **1a** to triplet phenyl nitrene **3a**.[12−14]

Theory predicts that singlet nitrene **1a** has an open-shell electronic structure and can be thought as a 1,3 biradical.[14−16]

Scheme 1

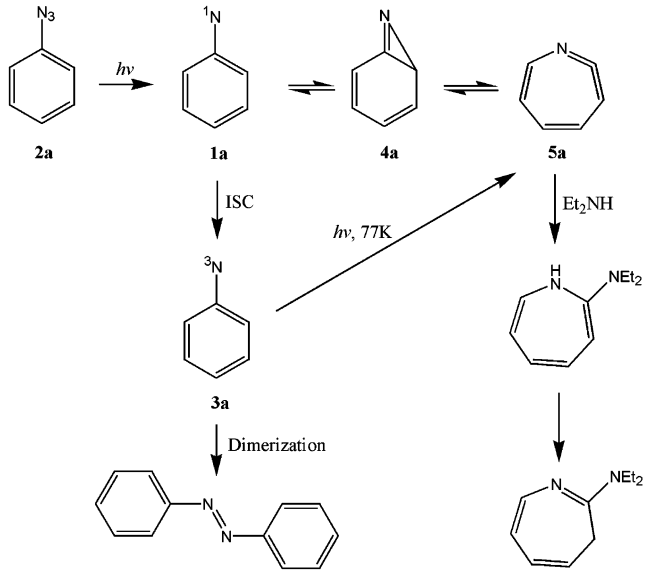

(1) Abramovitch, R. A.; Davis, B. A. *Chem. Rev.* **1964**, *64*, 149.
(2) (a) Scriven, E. F. V. In *Reactive Intermediates*; Abramovitch, R. A., Ed., Plenum: New York, 1982, Vol. 2, Chapter 1. (b) Smith, P. A. S. In *Azides and Nitrenes − Reactivity and Utility*; Scriven, E. F. V., Ed.; Academic Press Inc.: New York, 1984, Chapter 3.
(3) (a) Schuster, G. B.; Platz, M. S. *Adv. Photochem.* **1992**, *17*, 69. (b) Platz, M. S. *Acc. Chem. Rev.* **1995**, *28*, 487. (c) Borden, W. T.; Gritsan, N. P.; Hadad, C. M.; Karney, W. L.; Kemnitz, C. R.; Platz, M. S. *Acc. Chem. Rev.* **2000**, *33*, 765. (d) Gritsan, N. P.; Platz, M. S. *Adv. Phys. Org. Chem.* **2001**, *36*, 255.
(4) Greiss, P. *Philos. Trans. R. Soc. London* **1864**, *13*, 377.
(5) (a) Cai, S. X.; Glenn, D. J.; Gee, K. R.; Yan, M. D.; Cotter, R. E.; Reddy, N. L.; Weber, E.; Keana, J. F. W. *Bioconjugate Chem.* **1993**, *4*, 545. (b) Platz, M. S. *Photochem. Photobio.* **1997**, *65*, 193.
(6) Bayley, H.; Staros, J. V. In *Azides and Nitrenes − Reactivity and Utility*; Scriven, E. F. V. Ed., Academic Press Inc.: New York, 1984, Chapter 9.
(7) Cai, S. X.; Glenn, D. J.; Kanskar, M.; Wybourne, M. N.; Keana, J. F. W. *Chem. Mater.* **1994**, *6*, 1822.
(8) Meijer, E. W.; Nijhuis, S.; Vroonhoven, F. C. B. M. *J. Am. Chem. Soc.* **1988**, *110*, 7209.
(9) Nahar, P.; Wali, N. M.; Gandhi, R. P. *Anal. Biochem.* **2001**, *294*, 148.
(10) Cai, S. X.; Glenn, D. J.; Keana, J. F. W. *J. Org. Chem.* **1992**, *57*, 1299.
(11) Schrock, A. K.; Schuster, G. B. *J. Am. Chem. Soc.* **1984**, *106*, 5228.
(12) Gritsan, N. P.; Yuzawa, T.; Platz, M. S. *J. Am. Chem. Soc.* **1997**, *119*, 5059.
(13) Born, R.; Burda, C.; Senn, P.; Wirz, J. *J. Am. Chem. Soc.* **1997**, *119*, 5061.
(14) Gritsan, N. P.; Zhu, Z.; Hadad, C. M.; Platz, M. S. *J. Am. Chem. Soc.* **1999**, *121*, 1202.

10.1021/ja035833e CCC: $25.00

Compared to phenylcarbene[3b,15a] the biradical nature of **1a** facilitates its cyclization to benzazirine **4a**, which then rapidly undergoes a ring-expansion reaction to form didehydroazepine **5a** (Scheme 1).

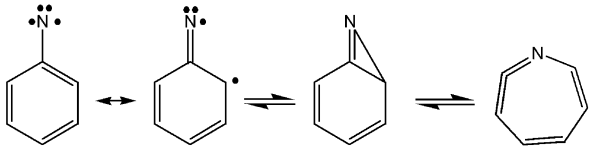

1a **4a** **5a**

Even though benzazirine **4a** has never been directly observed, the intermediacy of **4a** is supported by modern MO calculations[15,16] and by conventional chemical trapping experiments.[17] Photolysis of phenyl azide **2a** in ethanethiol produces ethylthioaniline, presumably from nucleophilic interception of **4a**.[17a]

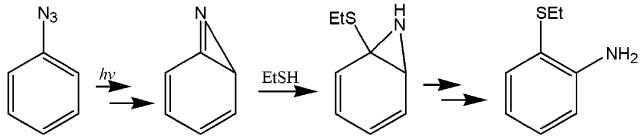

2a **4a**

Decomposition of phenyl azide **2a** at ambient temperature in amine containing solution generates 3H-azepines in good yield[18] via trapping of didehydroazepine **5a**.

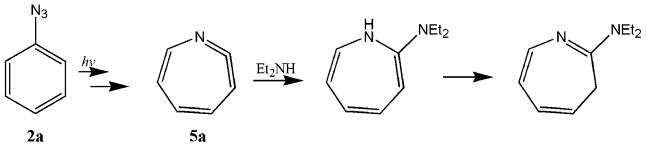

2a **5a**

Matrix isolation experiments performed at very low temperature,[19] time-resolved infrared (TRIR) studies at ambient temperature,[20] and LFP studies[12] provided direct observation of **5a**. Didehydroazepine **5a** has a characteristic broad and intense UV−vis absorption at 340 nm,[11,12,20] whose growth exhibits the same rate constant as the decay of singlet nitrene **1a**,[12] and an intense IR absorption at 1890 cm^{-1} attributed to the stretching of the ketenimine functional group.[19,20]

Sundberg and co-workers[21] discovered that ortho alkyl substituents direct the cyclization of the nitrene nitrogen away from the substituent.

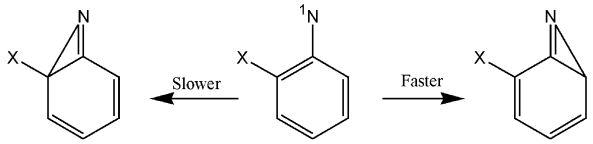

4' **1** **4**

X = CH_3

This laboratory has investigated a series of methyl substituted singlet phenylnitrenes using LFP methods.[22] A single ortho or para methyl group has no influence on the lifetime of the singlet aryl nitrene. However, two *ortho*-methyl groups extend the lifetime of 2,6-dimethylphenylnitrene to 12 ns at ambient temperature, and raises the energy barrier to rearrangement by 2 kcal/mol.[22] These results are in excellent agreement with Karney and Borden's calculations which indicate that steric strain increases upon cyclization of the singlet meta-xylyl nitrene to the corresponding azirine.[23−25,3d]

These results stimulated us to extend the steric effects to include di-ortho ethyl, isopropyl and *tert*-butyl substituents and herein we are pleased to report our results.

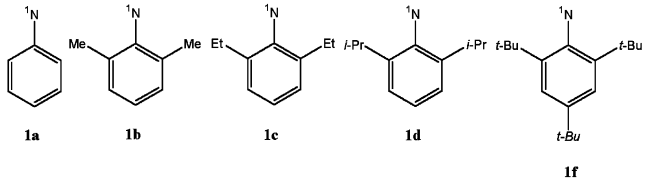

1a **1b** **1c** **1d** **1f**

II. Laser Flash Photolysis Studies

II.1 LFP of Phenyl Azides at 77K. The transient absorption spectrum of singlet phenylnitrene **1a** has been measured directly at ambient temperature[12] and at a lower temperature (150 K).[14] Other nitrenes, however, may not be directly observable at ambient temperature or even at 150 K by nanosecond spectroscopy. This led us to further decrease the reaction temperature.

Laser flash photolysis (LFP, 266 nm, 5 ns, 50 mJ) studies of **1a**−**1f** were performed in glassy 3-methylpentane at 77 K, in boiling liquid nitrogen. The data obtained with **1f** are representative. The spectrum recorded immediately after the laser flash (Figure 1A, solid line) is assigned to the open-shell singlet nitrene **1f**, and the transient spectrum formed at later times relative to the flash (Figure 1A, dashed line) is attributed to the triplet nitrene **3f**. Figure 1A illustrates that **1f** (346, 363 nm) and **3f** (313 nm) have distinct absorption spectra.

The 77 K LFP technique can also be utilized to directly measure the rate constant of intersystem crossing (k_{ISC}), which is based on the assumption that ISC is the dominant reaction of singlet phenylnitrenes at this temperature. As shown in Figure 1B, the variation in optical density as a function of time exhibits first-order kinetics at 363 and 313 nm. The growth of triplet phenylnitrene **3f** (313 nm) and the decay of singlet phenylnitrene **1f** (363 nm) exhibit the same rate constant, k_{ISC}.

The data obtained by LFP studies of several singlet and triplet phenylnitrenes at 77 K are summarized in Table 1.

II.2 LFP of 2,6-Diethyl and 2,6-Diisopropyl Phenyl Azide. The results obtained by LFP of 2,6-diisopropyl phenyl azide are very similar to the data reported with parent phenyl azide.[14]

(15) (a) Karney, W. L.; Borden, W. T. *J. Am. Chem. Soc.* **1997**, *119*, 1378. (b) Hrovat, D. A.; Waali, E. E.; Borden, W. T. *J. Am. Chem. Soc.* **1992**, *114*, 8698.
(16) Johnson, W. T. G.; Sullivan, M. B.; Cramer, C. J. *Int. J. Quantum Chem.* **2001**, *85*, 492.
(17) (a) Carroll, S. E.; Nay, B.; Scriven, E. F. V.; Suschitzky, H.; Thomas, D. R. *Tetrahedron Lett.* **1977**, 3175. (b) Younger, C. G.; Bell, R. A. *J. Chem. Soc., Chem. Commun.* **1992**, 1359.
(18) (a) Huisgen, R.; Vossius, D.; Appel, M. *Chem Ber.* **1958**, *91*, 1. (b) Huisgen, R.; Appl, M. *Chem. Ber.* **1958**, *91*, 12. (c) Doering, W. E.; Odum, R. A. *Tetrahedron* **1966**, *22*, 81.
(19) (a) Dunkin, I. R.; Lynch, M. A.; McAlpine, F.; Sweeney, D. *J. Photochem. Photobio. A: Chem.* **1997**, *102*, 207. (b) Hayes, J. C.; Sheridan, R. S. *J. Am. Chem. Soc.* **1990**, *112*, 5879. (c) Donnelly, T.; Dunkin, I. R.; Norwood, D. S. D.; Prentice, A.; Shields, C. J.; Thomson, P. C. P. *J. Chem. Soc., Perkin Trans. 2*, **1985**, 307. (d) Chapman, O. L.; LeRoux, J. P. *J. Am. Chem. Soc.* **1978**, *100*, 282.
(20) (a) Li, Y. Z.; Kirby, J. P.; George, M. W.; Poliakoff, M.; Schuster, G. B. *J. Am. Chem. Soc.* **1988**, *110*, 8092. (b) Shields, C. J.; Chrisope, D. R.; Schuster, G. B.; Dixon, A. J.; Poliakoff, M.; Turner, J. J. *J. Am. Chem. Soc.* **1987**, *109*, 4723
(21) Sundberg, R. J.; Suter, S. R.; Brenner, M. *J. Am. Chem. Soc.* **1972**, *74*, 513.
(22) Gritsan, N. P.; Gudmundsdottir, A. D.; Tigelaar, D.; Platz, M. S. *J. Phys. Chem. A* **1999**, *103*, 3458.

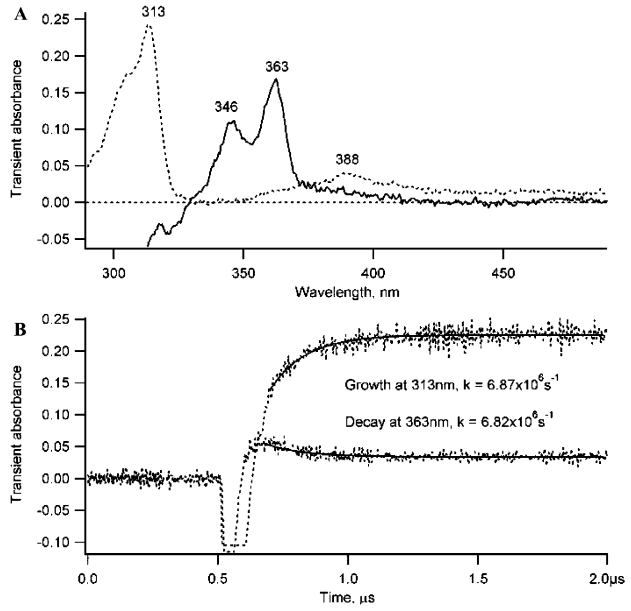

Figure 1. (A) Transient UV−visible spectra produced upon LFP (266 nm) of 2,4,6-tri-*tert*-butylphenyl azide in 3-methylpentane at 77 K. The solid line was observed over a window of 20 ns immediately after the laser flash; the dashed line was recorded over a window of 30 ns and 1 μs after the laser pulse. (B) The variation in optical density as a function of time at 363 nm (decay) and 313 nm (growth) following excitation of 2,4,6-tri-*tert*-butylphenyl azide in glassy 3-methylpentane at 77 K.

Table 1. Summary of LFP Data Obtained at 77 K

singlet nitrene	λ_{max} (nm)	k_{decay} (s^{-1})	triplet nitrene	λ_{max} (nm)	k_{growth} (s^{-1})
1a	349	3.8×10^6	**3a**	300	3.8×10^6
1c	350	8.4×10^6	**3c**	306	1.2×10^7
1d	360	9.3×10^6	**3d**	310	1.4×10^7
1f	346, 363	6.8×10^6	**3f**	313, 388	6.9×10^6

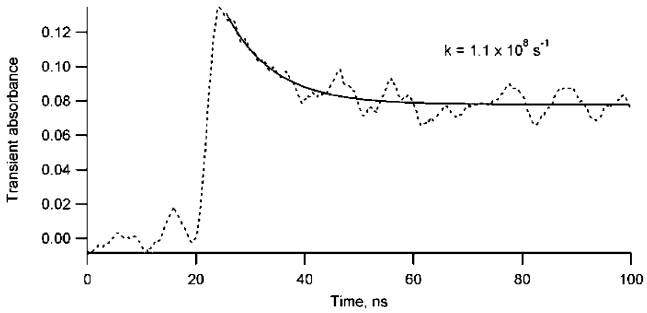

Figure 2. Variation in optical density as a function of time at 350 nm following excitation (266 nm, 150 ps, 10 mJ) of 2,6-diethylphenyl azide in pentane at ambient temperature.

LFP of 2,6-diethyl phenyl azide produces a short-lived transient absorption at 350 nm at ambient temperature.

The decay of transient absorption of singlet nitrene **1c** at 350 nm at ambient temperature is shown in Figure 2. This decay can be fit to an exponential function and solved to yield an observed rate constant k_{obs}. The lifetime of singlet nitrene **1c** is then determined from the reciprocal of k_{obs} to give $\tau = 9$ ns at ambient temperature. This is much longer than that of parent singlet phenylnitrene **1a** ($\sim$1 ns),[14] and is slightly shorter but close to that of singlet 2,6-dimethylphenylnitrene **1b** (12 ns).[22]

The transient spectrum of singlet nitrene **1c** could not be obtained directly at ambient temperature, as its lifetime is shorter

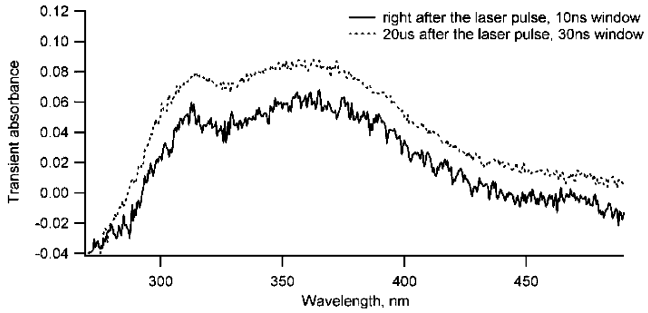

Figure 3. Transient UV−visible spectra produced upon LFP (266 nm) of 2,6-diethyl phenyl azide in pentane at ambient temperature.

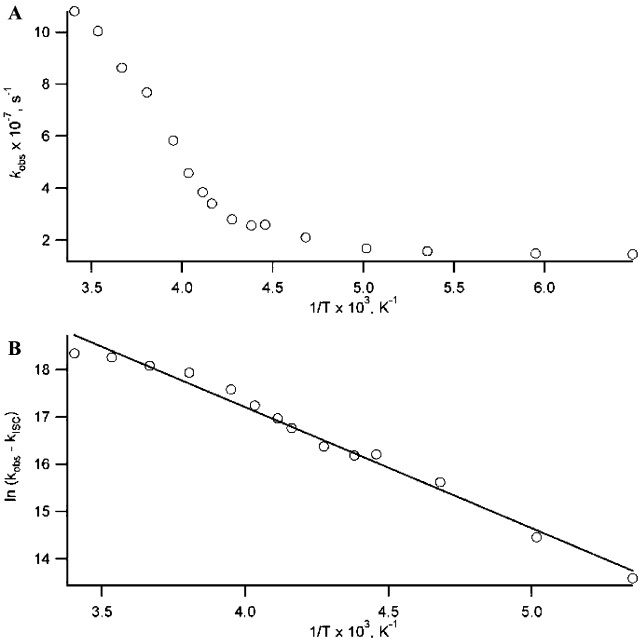

Figure 4. (A) A plot of k_{obs} versus $1/T$ and (B) Arrhenius plot of $\ln(k_{obs} - k_{ISC})$ versus $1/T$ for the decay of singlet nitrene **1c** in pentane.

than the time resolution of our instrument. Instead, the transient signal of the corresponding didehydroazepine **5c** was observed between 300 $\sim$ 400 nm with a maximum at around 360 nm (Figure 3). This spectrum greatly resembles that of parent system **5a**.[14]

LFP of **2c** in pentane at 193 K produces the transient absorption spectrum of Figure S4 (Supporting Information). This spectrum is significantly different from that at ambient temperature (Figure 3), and most resembles the spectrum observed in a frozen glass at 77 K with a 200 ns recording delay time (Figure S2, dashed line).

The temperature dependence of the observed rate constant, k_{obs}, for the decay of singlet nitrene **1c** is examined and the results are listed in Table S1 (Supporting Information). The magnitude of k_{obs} decreases as the temperature decreases until about 170 K, whereupon a limiting value is reached (Figure 4A). This is similar to the trend observed with singlet phenylnitrene **1a**[14] and a series of its derivatives.[3c,22,24,26]

The temperature independent rate constant observed at low temperature, which is determined to be $(1.5 \pm 0.1) \times 10^7$ s^{-1}, is associated with the rate constant of ISC to the lowest triplet state (k_{ISC}). Following our studies of parent singlet phenylnitrene[14] and other substituted phenylnitrenes,[22,24,26] it is assumed that k_{obs} has two components: the rate constant of rearrangement

(k_R) and the rate constant of intersystem crossing (k_{ISC})

$$k_{obs} = k_R + k_{ISC} \quad (1)$$

Assuming further that k_{ISC} does not vary with temperature in solution over the range of this study allows deduction of the rate constant of rearrangement (k_R).[3c,22,24,26] Arrhenius treatment of k_R, represented as ($k_{obs} - k_{ISC}$), is depicted in Figure 4B, where a linear relationship is found with a regression coefficient of 0.992 for the least-squares linear fitting. Thus, the deduced Arrhenius parameters for singlet nitrene **1c** to rearrangement have an activation energy (E_a) of 5.2 ± 0.5 kcal/mol, and a preexponential factor (A) of $10^{12.1\pm0.5}$ s^{-1}. This energy barrier is similar to that of parent phenylnitrene **1a** (5.6 ± 0.3 kcal/mol)[14] but is significantly smaller than that of 2,6-dimethylphenylnitrene **1b** (7.0 ± 0.3 kcal/mol).[22] Furthermore, the preexponential factor for **1c** to rearrangement is about 1 order of magnitude smaller than those of **1a** and **1b** ($10^{13.0\sim13.1\pm0.3}$ s^{-1}).[14,22]

One can imagine that compensating experimental errors in the activation energies and preexponential terms may obscure or falsely amplify trends in the barrier heights.[3d] For this reason, a fixed preexponential value of $10^{13.0\sim13.4}$ s^{-1} or a fixed intercept of $\ln(10^{13.0\sim13.4})$ was applied to the Arrhenius treatment of $\ln k_R$ versus $1/T$, similar to that of Figure 4B, and this treatment gives a larger E_a (6.2∼6.7 kcal/mol) but a poorer regression coefficient (0.965) than those derived from Figure 4B. Nevertheless, this energy barrier is still lower than, but closer to, that of **1b**.

LFP (266 nm, 150 ps, 10 mJ) of 2,6-diisopropylphenyl azide **2d** in pentane at 193 K produces the transient absorption spectrum of Figure S5 (Supporting Information). This spectrum resembles that observed in a glass at 77 K 300 ns after the laser pulse and is attributed to the triplet nitrene **3d**. At a time resolution of 100 ns, our optical multichannel analyzer could not detect singlet nitrene **1d** at 193 K in the condensed phase. Furthermore, no significant didehydroazepine transient absorption was detected at this temperature either.

At ambient temperature, LFP of **2d** produces a broad transient absorption with maximum at 360 nm (similar to Figure 3) assigned to didehydroazepine **5d**, and the decay of transient absorption of singlet nitrene **1d** is not observable. The band at 310 nm is likely due to the triplet nitrene **3d**. Thus, the lifetime of **1d** must be shorter than 5 ns at ambient temperature. However, the decay of transient absorption of singlet nitrene **1d** at 360 nm, is observed at 260 K (Figure S6) or lower temperatures. This decay trace can be fit to an exponential function and solved to yield observed rate constant, k_{obs}, of 1.6 × 10^8 s^{-1}, which corresponds to a lifetime of ∼6 ns at 260 K. At this temperature, the lifetimes of singlet phenylnitrene **1a**, its 2,6-dimethyl analogue **1b**, and 2,6-diethyl analogue **1c** are about 3,[14] 40,[22] and 13 ns (Table S1), respectively. The lifetime

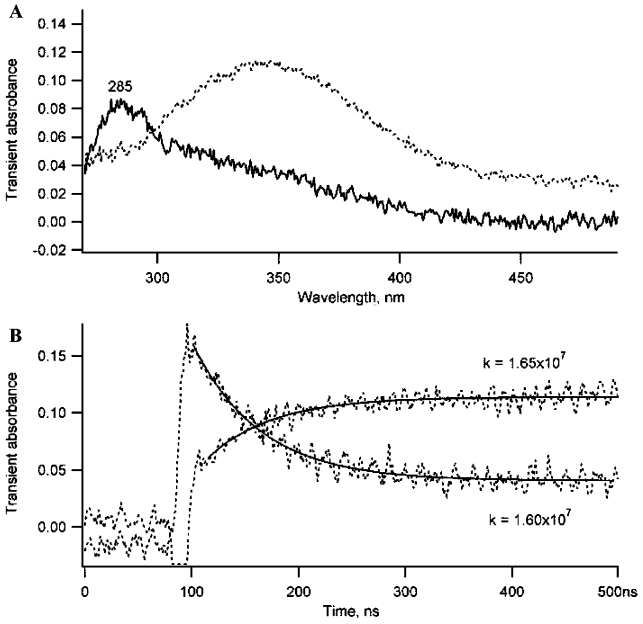

Figure 5. (A) Transient UV−visible spectra produced upon LFP (266 nm) of 2,4,6-tri-*tert*-butylphenyl azide in pentane at ambient temperature. The solid line was observed over a window of 10 ns just after the laser flash; the dashed line was recorded over a window of 30 ns and 10 μs after the laser pulse. (B) The variation in optical density as a function of time at 285 nm (decay) and 350 nm (growth) following excitation of 2,4,6-tri-*tert*-butylphenyl azide in pentane at ambient temperature.

of diisopropyl nitrene **1d** is twice as large as singlet phenylnitrene **1a**, but less than half of that of diethylphenylnitrene **1c** at 260 K.

II.3 LFP of 2,4,6-tri-*tert*-Butylphenyl Azide in Fluid Solution. LFP (266 nm) of 2,4,6-tri-*tert*-butylphenyl azide **2f** in pentane, at ambient temperature, produces the transient absorption spectra of Figure 5A. The transient absorption of singlet nitrene **1f** at 346 and 363 nm could not be observed at ambient temperature presumably due to its very short lifetime under these conditions. Instead, a transient species, which absorbs strongly around 285 nm, with a long tail extending to about 400 nm, is observed immediately after the laser pulse. This transient spectrum is significantly different from that of singlet nitrene **1f** and triplet nitrene **3f**. Its maximum absorption exhibits a blue shift of 30 nm relative to that of **3f**, and it does not display the structured bands at 363 and 346 nm as does singlet nitrene **1f** observed at 77 K. The carrier of 285 nm transient absorption will be assigned to benzazirine **4f** on the basis of its kinetic and spectroscopic properties (vide infra).

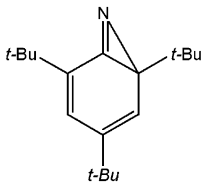

4f

Note that direct observations of benzazirines are rare, particularly in the liquid phase. Other cases are the azirines produced by photolysis of *ortho*-biphenyl azide,[27a] 2,6-difluoro and pentafluorophenyl azide,[27b] and 1-naphthyl azide.[27c]

Hundreds of nanoseconds after the laser flash, the 285 nm transient absorption vanishes and a new transient absorption

(23) (a) Poe, R.; Schnapp, K.; Young, M. J. T.; Grayzar, J.; Platz, M. S. *J. Am. Chem. Soc*. **1992**, *114*, 5054. (b) Schnapp, K. A.; Poe, R.; Leyva, E.; Soundararajan, N.; Platz, M. S. *Bioconjugate Chem.* **1993**, *4*, 172. (c) Zhai, H. B.; Platz, M. S. *J. Phys. Org. Chem.* **1997**, *10*, 22. (d) Gritsan, N. P.; Zhai, H. B.; Yuzawa, T.; Karweik, D.; Brooke, J.; Platz, M. S. *J. Phys. Chem. A* **1997**, *101*, 2833.
(24) Gritsan, N. P.; Gudmundsdottir, A. D.; Tigelaar, D.; Zhu, Z.; Karney, W. L.; Hadad, C. M.; Platz, M. S. *J. Am. Chem. Soc*. **2001**, *123*, 1951.
(25) Karney, W. L.; Borden, W. T. *J. Am. Chem. Soc*. **1997**, *119*, 3347.
(26) Gritsan, N. P.; Likhotvorik, I.; Tsao, M.-L.; Çelebi, N.; Platz, M. S.; Karney, W. L.; Kemnitz, C. R.; Borden, W. T. *J. Am. Chem. Soc*. **2001**, *123*, 1425.

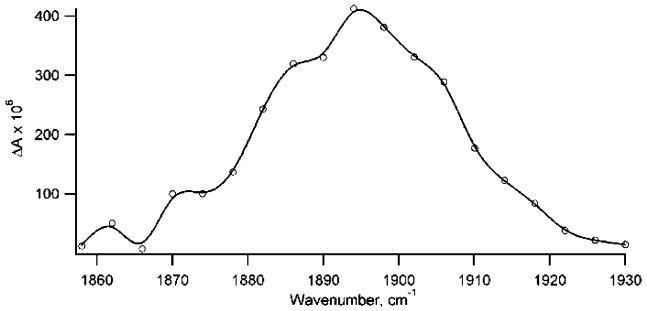

Figure 6. Transient IR spectrum produced upon LFP (240 nm) of 2,4,6-tri-*tert*-butylphenyl azide in acetonitrile at ambient temperature. The spectrum was recorded over a window of 1 μs immediately after the laser flash.

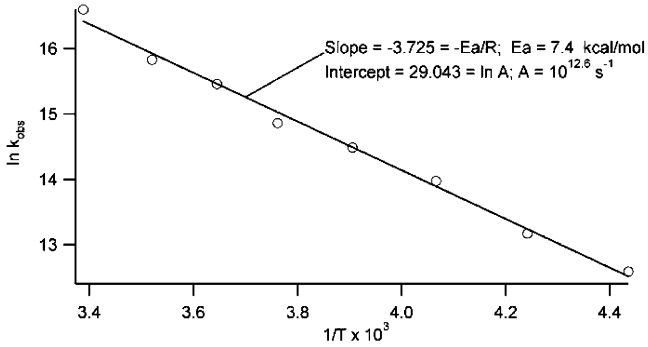

Figure 7. Arrhenius plot for the temperature dependence of the observed decay rate constant k_{obs} at 290 nm upon LFP (266 nm) of 2,4,6-tri-*tert*-butylphenyl azide in pentane.

Scheme 2

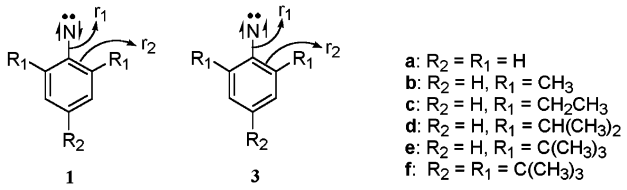

appears which absorbs broadly and intensely at 300∼440 nm with a maximum of 350 nm. Its lifetime is more than tens of microseconds (Figure 5A). This longer-lived transient species can be identified as didehydroazepine **5f** based on the similarity of its UV−vis absorption to the spectrum generated from phenyl azide[12] and its derivatives (Figure 3). The carrier of the 285 nm absorption band must decay to form didehydroazepine **5f**, consistent with its assignment to benzazirine **4f**.

To further support the assignment of didehydroazepine **5f**, LFP of azide **2f** was investigated with infrared detection. Figure 6 depicts the time-resolved infrared (TRIR) spectrum produced upon LFP (240 nm) of 2,4,6-tri-*tert*-butylphenyl azide (**2f**) in acetonitrile at ambient temperature. Excitation light of 240 nm was chosen instead of 266 nm because **2f** absorbs more strongly at the shorter wavelength and 240 nm is the shortest accessible excitation wavelength of the TRIR spectrometer. The spectrum of Figure 6 reveals that the longer-lived transient species absorbs strongly at 1894 cm^{-1}, a characteristic IR absorption of the ketenimine functional group. This IR absorption greatly resembles that of didehydroazepine generated by LFP of phenyl azide.[20]

To explore the lifetime of the carrier of short-lived 285 nm transient absorption and the connection of this species with didehydroazepine **5f**, kinetic studies were performed at selected wavelengths as shown in Figure 5B. It was found that the disappearance of the transient absorption at 285 nm and the formation of the 350 nm transient signal are exponential. The observed rate constants, k_{obs}, of both processes are equal within experimental error demonstrating that these two transient species are connected by a common mechanistic step. Furthermore, the lifetime of the carrier of the 285 nm absorbing species, deduced from the reciprocal of k_{obs}, is 62 $\pm$ 2 ns in pentane at ambient temperature (Figure 5B).

LFP (266 nm) of 2,4,6-tri-*tert*-butylphenyl azide in pentane at 193 K produces the transient absorption spectrum of Figure S7 (Supporting Information). The transient spectrum observed at 193 K shows exactly the same features as that obtained at ambient temperature immediately after the laser flash (Figures 5A); however, the lifetime of the 285 nm transient species extends to the microsecond time scale at the lower temperature.

The temperature dependence of the observed rate constant, k_{obs}, for the decay of transient absorption at 285 nm is examined and the results are listed in Table S2 (Supporting Information). The magnitude of k_{obs}, which follows the Arrhenius equation, decreases as the temperature decreases. An Arrhenius treatment of the k_{obs} data is presented in Figure 7. Unlike singlet phenylnitrene in which a curved Arrhenius plot was observed for its decay rate constants, Figure 7 displays an excellent linear relationship between ln k_{obs} and $1/T$ over the entire temperature range of the study.

Following a least-squares linear correlation of the data, the activation energy E_a and preexponential factor A for the decay of 285 nm transient are found to be $E_a = 7.4 \pm 0.2$ kcal/mol and $A = 10^{12.6\pm0.2}$ s^{-1}.

III. Computational Chemistry

III.1 Singlet−Triplet Splitting of Substituted Phenylnitrenes. The electronic structures of a series of *ortho*-alkylated phenylnitrenes (Scheme 2) were investigated using computational methods. The geometries of these nitrenes were optimized using the complete active space self-consistent field (CASSCF) methodology[28] with the 6-31G* basis set[29] in which five d-type (5D) functions were employed. Due to free rotation of C−C bond(s) in the alkyl substituents, several rotational isomers can be found in these nitrenes. However, only the most stable isomers were chosen and studied in detail with the exception of **3f**. An isomer of **3f** with C_s symmetry was used as a representative molecule instead of the most stable isomer that does not have any molecular symmetry. This analysis was performed because the C_s point group can be used to great advantage in electronic structure calculations, and this C_s isomer is geometrically and energetically similar to the most stable one. The triplet state of **3f** with C_s symmetry is only 0.02 kcal/mol above the most stable isomer at the B3LYP/6-31G* level of theory. Moreover, a vibrational frequency calculation on **3f** with

(27) (a) Tsao, M.-L.; Gritsan, N.; James, T. R.; Platz, M. S.; Hrovat, D. A.; Borden, W. T. *J. Am. Chem. Soc.* **2003**, *125*, in press. (b) Morawietz, J.; Sander, W. *J. Org. Chem.* **1996**, *61*, 4351. (c) Dunkin, I. R.; Thomson, P. C. P. *J. Chem. Soc., Chem. Commun.* **1980**, 499.

(28) (a) Roos, B. O. In *Ab Initio Methods in Quantum Chemistry*; Lawley, K. P., Ed.; Wiley: New York, 1987; Vol.2, p 399. (b) Roos, B. O. *Adv. Chem. Phys.* **1987**, *69*, 339. (c) Roos, B. O. *Int. J. Quantum Chem. Symp.* **1980**, *14*, 175.

(29) Hariharan, P. C.; Pople, J. A. *Theor. Chim. Acta* **1973**, *28*, 213.

Table 2. Calculated Absolute Energies (Hartrees) of Triplet Nitrenes 3a∼3f and Singlet−Triplet Energy Gaps (kcal/mol) of Singlet Nitrenes 1a∼1f Using the CASSCF, CASPT2, and DFT Computational Methods

	CASSCF[a]		CASPT2[b]		DFT[c]	
substituents	3	ΔE_{ST}	3	ΔE_{ST}	3	ΔE_{ST}
a	−284.594522	17.88	−285.399723	19.52	−286.389598	15.16
b	−362.668826	16.04	−363.745850	17.82	−365.049901	13.67
c	−440.736211	16.36	−442.080415	17.89	−443.698143	13.74
d	−518.799366	16.15	−520.417320	17.93	−522.344683	13.72
e	−596.854703	15.47	−598.752589	17.42	−600.985105	13.27
f	−752.988064	15.31	−755.430741	17.08	−758.284476	13.05

[a] CASSCF(8,8)/6-31G* level of theory. [b] CASPT2(8,8)/6-31G*//CASSCF(8,8)/6-31G* level of theory. [c] UB3LYP/6-311+G(2d,p)//UB3LYP/6-31G* level of theory.

C_s symmetry at this level verifies its nature as minimum on the potential energy surface rather than a transition state.

Phenylnitrene (**1a** and **3a**) along with 2,6-dimethyl (**1b** and **3b**), 2,6-diisopropyl (**1d** and **3d**), and 2,6-di-*tert*-butyl (**1e** and **3e**) phenylnitrenes are C_{2v} symmetric, while 2,4,6-tri-*tert*-butylphenyl nitrene (**1f** and **3f**) has C_s symmetry. As for 2,6-diethylphenyl nitrene (**1c** and **3c**), two isomers are found to have the lowest energies. The most stable isomer shows C_2 symmetry, whereas the other one has C_s symmetry. The energy difference between these two isomers is smaller than 0.1 kcal/mol.

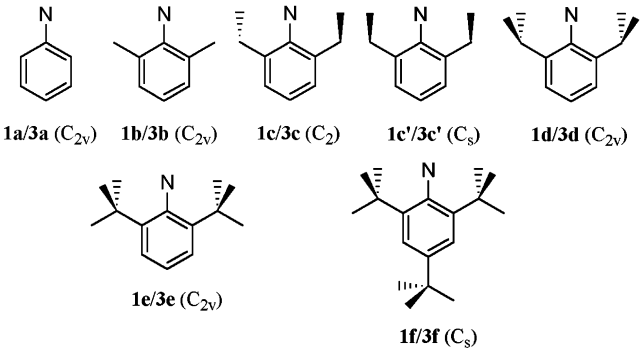

Geometric and thermodynamic information concerning these nitrenes are listed in Table S3 (Supporting Information) and Table 2. Table S3 reveals that the C−N bond length (r_1) in singlet nitrenes **1a**∼**1f** is 0.05∼0.06 Å shorter than in their triplet states, and the adjacent C−C bond length (r_2) in singlet nitrenes **1a**∼**1f** is about 0.05 Å longer than in the triplet states. This demonstrates the biradical character of the singlet nitrenes found in previous calculations.[14−16] There is very little influence of substituent present in the geometric data.

The calculated singlet−triplet energy gap, ΔE_{ST}, with the CASSCF(8,8)/6-31G* method is given in Table 2. To include dynamic electron correlation in the multiconfiguration calculations, CASPT2[30] energies were determined for CASSCF optimized geometries using the CASSCF wave functions as a reference. These CASPT2 energies are also listed in Table 2. Both CASSCF and CASPT2 calculations show that alkyl substitutions lower the singlet−triplet energy gap by 1.5∼2.5 kcal/mol. However, the bulkiness of alkyl groups has very little influence on ΔE_{ST}.

The singlet−triplet splitting of nitrenes **1a**∼**1f** was also studied by density functional theory (DFT) with Becke's three parameter hybrid functional using the LYP correlation functional (B3LYP).[31] Geometries of singlet nitrenes **1a**∼**1f** as well as triplet nitrenes **3a**∼**3f** were fully optimized using the UB3LYP/6-31G* (6D) method, and their single-point energy calculations were performed with the extended 6-311+G(2d,p) basis set[32] for the UB3LYP/6-31G* optimized geometries. The results are listed in Table 2 as well.

Because singlet nitrenes **1a**∼**1f** have open-shell electronic structures the DFT method failed to describe these broken symmetry systems correctly. However, the energy of the broken-symmetry unrestricted DFT wave function, $E_{50:50}$, is best interpreted as a 50:50 mixture of triplet E_T and singlet E_S, for which the $<S^2>$ value is ∼ 1.0.[16,33,34] Thus, the DFT energy of the singlet state can be estimated by this sum method[16,33,34] as

$$E_S = 2 * E_{50:50} - E_T \qquad (2)$$

Compared to the singlet−triplet splitting calculated by CASSCF and CASPT2 (Table 2), DFT with the sum method underestimates ΔE_{ST} by 2∼4 kcal/mol. However, this deviation is independent of substituent; that is, the trends in the singlet−triplet splitting as a function of substitution are similar between the DFT sum method and the CASSCF and CASPT2 calculations. This is consistent with the published results of *meta* and *para* substitution effects on the electronic state energies of phenylnitrene.[16]

III.2 Intramolecular Rearrangement of Singlet Phenylnitrene. The intramolecular rearrangement of singlet phenylnitrene **1** proceeds by a two-step process.[15] The first step is cyclization of phenylnitrene to form benzazirine **4**, and the second step is ring enlargement of **4** to give didehydroazepine **5** (Scheme 3). To explore the potential energy surface of these processes for singlet nitrenes **1a**∼**1f**, stationary points are examined using modern MO theory.

Because the first cyclization step involves both open-shell (**1a**∼**1f**) and closed-shell (**4a**∼**4f**) singlet species, the DFT method alone could not answer this question properly as described previously. Therefore, CASSCF, CASPT2, and DFT/CASPT2 combination methods are used to explore the cyclization step. For CASSCF and CASPT2 methods, the geometries of **1a**∼**f**, **4a**∼**f** and the transition states connecting between them (**TS_{1-4} a**∼**f**) were optimized at the CASSCF(8,8)/6-31G* level of theory, and then the CASPT2 energies of these CASSCF geometries were determined using the CASSCF wave functions as a reference. These calculations produce the geometric information of Tables S4−S7 (Supporting Information), and yield the relative energies of Table S8. Note that due to severe problems of orbital rotations during the CASSCF geometry optimization of **TS_{1-4}f**, calculations of this molecule could not be completed with the CASSCF method, and the CASPT2 calculation of **TS_{1-4}e** was too expensive to perform with our

(30) (a) Anderson, K.; Malmqvist, P.-Å.; Roos, B. O.; Sadlej, A. J.; Wolinski, K. *J. Phys. Chem.* **1990**, *94*, 5483. (b) Anderson, K.; Malmqvist, P.-Å.; Roos, B. O. *J. Chem. Phys.* **1992**, *96*, 1218. (c) Anderson, K.; Roos, B. O. *Int. J. Quantum Chem.* **1993**, *45*, 591.

(31) (a) Becke, A. D. *J. Chem. Phys.* **1993**, *98*, 5648. (b) Lee, C.; Yang, W.; Parr, R. G. *Phys. Rev. B* **1988**, *37*, 785. (c) Miehlich, B.; Savin, A.; Stoll, H.; Preuss, H. *Chem. Phys. Lett.* **1989**, *157*, 200.

(32) (a) Frisch, M. J.; Pople, J. A.; Binkley, J. S. *J. Chem. Phys.* **1984**, *80*, 3265. (b) Clark, T.; Chandrasekhar, J.; Schleyer, P. v. R. *J. Comput. Chem.* **1983**, *4*, 294.

(33) Cramer, C. J. *Essentials of Computational Chemistry − Theories and Models*; Wiley: New York, 2002.

(34) (a) Ziegler, T.; Rauk, A.; Baerends, E. J. *Theor. Chim. Acat* **1977**, *43*, 261. (b) Cramer, C. J.; Dulles, F. J.; Giesen, D. J.; Almlöf, J. *Chem. Phys. Lett.* **1995**, *245*, 165.

Scheme 3

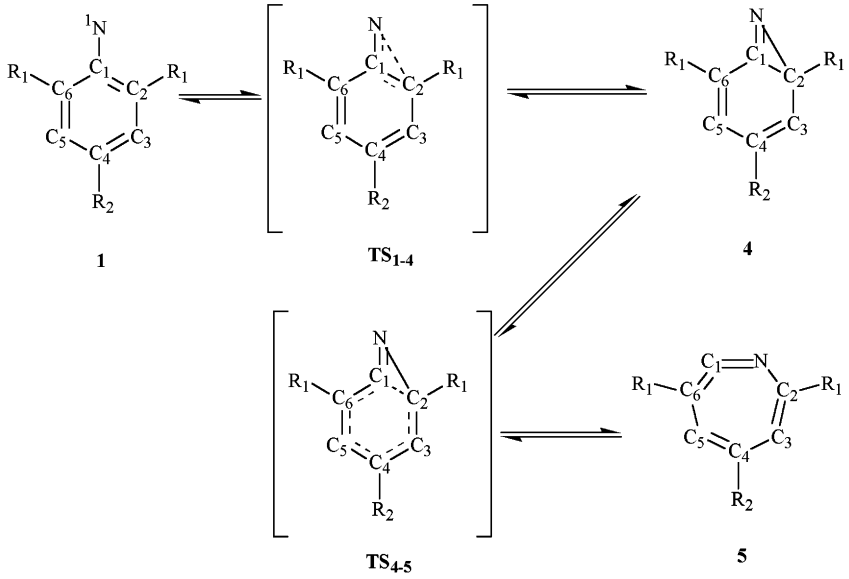

a: $R_2 = R_1 = H$
b: $R_2 = H$, $R_1 = CH_3$
c: $R_2 = H$, $R_1 = CH_2CH_3$
d: $R_2 = H$, $R_1 = CH(CH_3)_2$
e: $R_2 = H$, $R_1 = C(CH_3)_3$
f: $R_2 = R_1 = C(CH_3)_3$

computational resources. Regarding the DFT/CASPT2 method, the geometries of triplet nitrenes **3a**∼**3f** and singlet species **4a**∼**4f** and $\mathbf{TS_{1-4}}$**a**∼**f** were optimized at either the B3LYP or UB3LYP level of theory for closed-shell and open-shell species, respectively, with the 6-31G* basis set in which six Cartesian d functions (6D) were employed. Frequency calculations were also performed at the same computational level to examine the number of imaginary frequencies, and to obtain the zero-point vibrational energy (ZPE) corrections. Single-point energy calculations were conducted with an extensive 6-311+G(2d,p) basis set for the (U)B3LYP/6-31G* optimized geometries. The energies of $\mathbf{TS_{1-4}}$ and **4** relative to triplet nitrenes **3** at the B3LYP/6-311+G(2d,p)//B3LYP/6-31G* + ZPE level of theory will be denoted as ΔE_{DFT}. Combining ΔE_{DFT} with the CASPT2 singlet−triplet energy gap (ΔE_{ST}) of Table 2, the relative energies $\Delta E_{DFT/CASPT2}$ of $\mathbf{TS_{1-4}}$ and **4** to singlet nitrenes **1** can be deduced from eq 3 as

$$\Delta E_{DFT/CASPT2} = \Delta E_{DFT} - \Delta E_{ST} \qquad (3)$$

The observed geometric data from the DFT method are listed in Tables S4-S7 with the CASSCF result, and the DFT/CASPT2 energies are given in Table S8 and Figure 8.

The second step of the rearrangement reaction involves only closed-shell singlet species. Thus, DFT is reasonably expected to be accurate for computing the properties of stationary points of the second step. The geometries of **4**, **5**, and $\mathbf{TS_{4-5}}$, the transition states connecting **4** and **5**, were fully optimized at the B3LYP/6-31G* level. Some selective bond lengths in these species are listed in Tables S4-S7. Zero-point energies at the B3LYP/6-31G* level and single-point energies with the 6-311+G-(2d,p) basis set were calculated for the B3LYP/6-31G* optimized geometries. These energies along with the energies of **5** and $\mathbf{TS_{4-5}}$ relative to **4** at the B3LYP/6-311+G(2d,p)// B3LYP/6-31G*+ZPE level are given in Table S9 (Supporting Information). Didehydroazepines **5a**∼**f** are found to be 7.1∼8.8 kcal/mol more stable than their corresponding benzazirines **4a**∼**f**. Moreover, the activation energy of this step is affected by the nature of alkyl substituents: the bulkier the alkyl substituents, the larger the activation energy (Table S9, Figure 9).

The DFT/CASPT2 energies relative to the singlet nitrenes **1** for stationary points involved in the rearrangement of phenylnitrenes **1a**∼**f** are derived from the deduction of their singlet−triplet splitting (ΔE_{ST}) from their DFT energies relative to triplet nitrenes **3** (ΔE_{DFT}) as shown in eq 3. These results are given in Figure 8. In Figure 9 these DFT/CASPT2 relative energies are shifted to position benzazirines **4** at zero so that the second step of the rearrangement can be clearly visualized. Figures 8 and 9 show that the bulkiest substituent, *tert*-butyl, dramatically reduces the energy barrier of the first cyclization step and raises the barrier of the second ring-expansion step.

To understand the origin of the alkyl substituent effects, the intramolecular rearrangement of phenylnitrenes with 2-methyl **1g**, 2-isopropyl **1h**, 2-*tert*-butyl **1i**, and 4-*tert*-butyl **1j** substituents are investigated computationally using the same theoretical methods performed for dialkyl substituted analogues. At first, singlet−triplet energy gaps of **1g**∼**j** were determined using the CASSCF(8,8)/6-31G* geometry optimizations followed by CASPT2(8,8)/6-31G* single-point energy calculations. Second, DFT energies of all stationary points involved in the rearrangement of **1g**∼**j** (Scheme 4) were calculated using the B3LYP/6-311+G(2d,p)//B3LYP/6-31G* + ZPE method. Finally, the DFT/CASPT2 relative energies to singlet nitrenes **1** for these stationary points are deduced from eq 3. These energies are given in Table S10 (Supporting Information) and Figure 10,

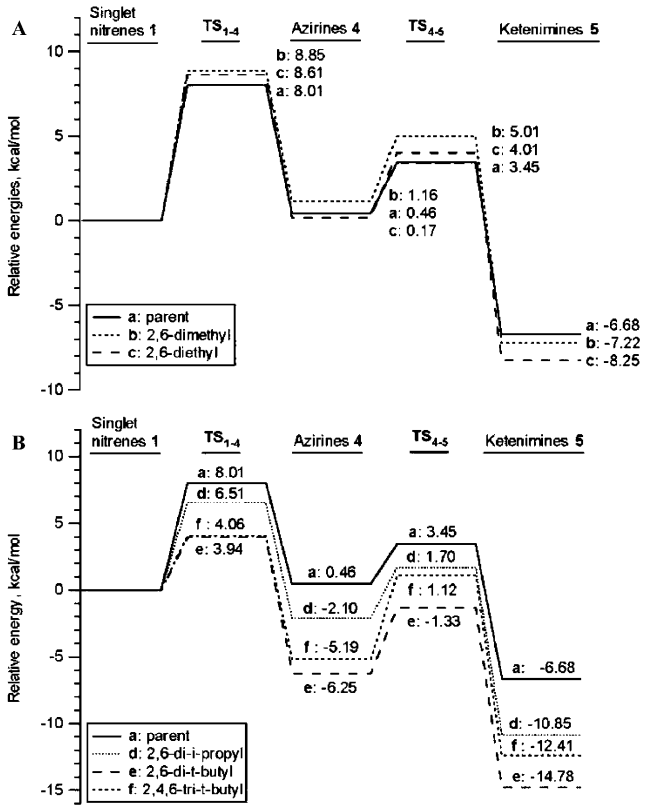

Figure 8. DFT/CASPT2 energies relative to singlet nitrenes **1** for species involved in the rearrangement of (A) phenylnitrene **1a**, 2,6-dimethylphenylnitrene **1b**, and 2,6-diethylphenyl nitrene **1c** and (B) 2,6-diisopropylphenylnitrene **1d**, 2,6-di-*tert*-butylphenyl nitrene **1e** and 2,4,6-tri-*tert*-butylphenylnitrene **1f**.

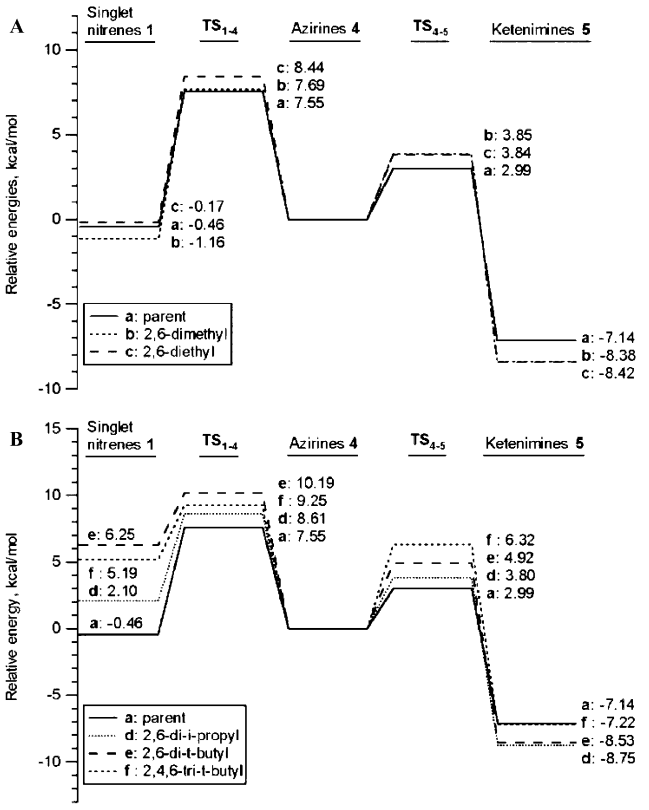

Figure 9. DFT/CASPT2 energies relative to benzazirines **4** for species involved in the rearrangement of (A) phenylnitrene **1a**, 2,6-dimethylphenylnitrene **1b**, and 2,6-diethylphenyl nitrene **1c** and (B) 2,6-diisopropylphenylnitrene **1d**, 2,6-di-*tert*-butylphenyl nitrene **1e** and 2,4,6-tri-*tert*-butylphenylnitrene **1f**.

along with those of unsubstituted phenylnitrene **1a** for comparison. Note that cyclization of nitrenes **1g**∼**i** might proceed toward or away from the alkyl substituent. Inspection of the data in Table S10 reveals that the energy barriers to cyclization away from the alkyl substituents are, unsurprisingly, smaller than those to cyclization toward them and are diminished as the size of the alkyl group increases. Regarding the second ring-expansion step, a *tert*-butyl substituent on either *ortho* (for the mode of away from substituent) or *para* position dramatically raises the barrier for this process. The DFT/CASPT2 energies relative to singlet nitrenes **1** (Figure 10A) and to benzazirine **4** (Figure 10B) give a much clearer picture of the effects of the *tert*-butyl substituent.

The relative energies of a series of monomethyl, dimethyl, mono-*tert*-butyl, and di-*tert*-butyl substituted benzazirines and didehydroazepines were calculated using the B3LYP/6-311+G-(2d,p)//B3LYP/6-31G* method with correction of the unscaled B3LYP/6-31G* ZPE differences. The results are presented in Figures 11−14. The most stable structure of the monomethylated benzazirines is the 2-methyl derivative, followed by the 5-methyl derivative. Consequently, the most stable of the dimethylated benzazirines is the 2,5-dimethyl derivative (Figure 11). The benzazirine (1,5-dimethyl substitution) derived from the cyclization of the *ortho*,*ortho*-dimethylphenylnitrene is ca. 0.49 kcal/mol less stable than its 2,5-dimethyl analogue.

For the benzazirines with mono-*tert*-butyl substitution, the most favorable structure is the 5-*tert*-butyl derivative (Figure 12). The next most stable structure is the 1-substituted analogue, which is 1.2 kcal/mol higher in energy than the 5-*tert*-butyl isomer. As predicted by analogy to the monosubstituted species, the most stable structure of the benzazirines with two *tert*-butyl substitutions is the 1,5-di-*tert*-butylbenzazirine (Figure 12), an intermediate derived from the cyclization of the *ortho*,*ortho*-di-*tert*-butylphenylnitrene. Other members of the di-*tert*-butyl substituted benzazirines are 0.7∼4.3 kcal/mol higher in energy than the 1,5-di-*tert*-butylbenzazirine.

Regarding the methylated and *tert*-butylated didehydroazepines, the methyl substituent prefers the 7-carbon position, followed by 4-carbon and then 3-carbon, while the *tert*-butyl group favors the 7-carbon position, followed by 3-carbon and then 4-carbon position. Both methyl and *tert*-butyl substituents significantly disfavor the 5- and 6-carbon positions (Figures 13 and 14).

IV. Discussion

The observed absorption maxima of **1a**, **1c**, **1d**, and **1f** at 349, 350, 360, and 363 nm, respectively, and those of **3a**, **3c**, **3d**, and **3f** at 300, 306, 310, and 313 nm, respectively, reveal only small substituent effects of alkyl groups on the λ_{max} of the transient absorption of singlet and triplet phenylnitrenes. Both **1f** and **3f** show a small red shift (∼13 nm) relative to the parent nitrenes **1a** and **3a**. Singlet nitrenes absorb UV−vis light with a significant red shift (∼50 nm) relative to their triplet states.[14]

As to the calculated singlet−triplet energy gap ΔE_{ST}, CASSCF, CASPT2, and DFT methods predict that the presence of alkyl substituents will lower the ΔE_{ST} by 1.5∼2.5 kcal/mol, but there is only a small influence due to the size of the alkyl groups (Table 2). Photoelectron spectroscopy of the anion of **1a** reveals a ΔE_{ST} value of 18 kcal/mol.[35]

Scheme 4

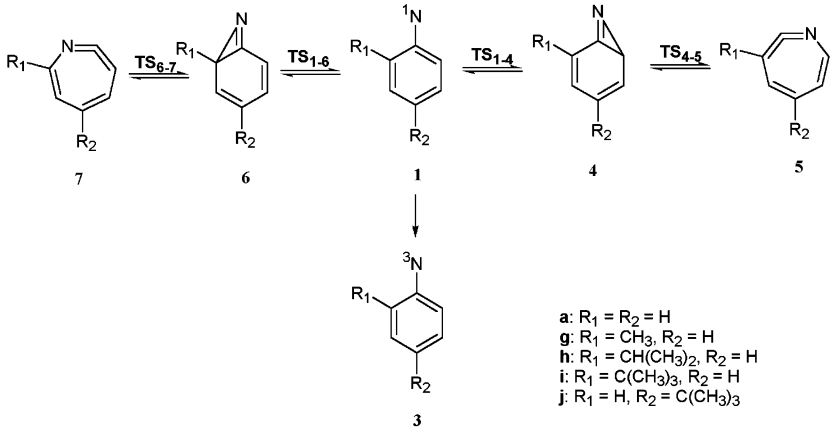

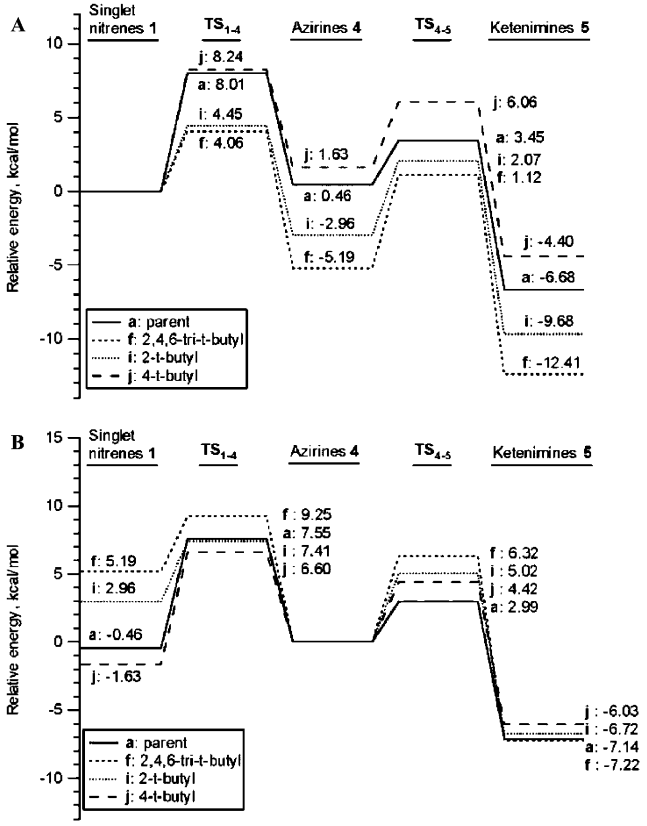

Figure 10. DFT/CASPT2 energies of species involved in the rearrangement of phenyl nitrene **1a**, 2,4,6-tri-*tert*-butylphenylnitrene **1f**, 2-*tert*-butylphenylnitrene **1i**, and 4-*tert*-butyl- phenylnitrene **1j** (A) relative to singlet nitrenes **1** and (B) relative to benzazirines **4**.

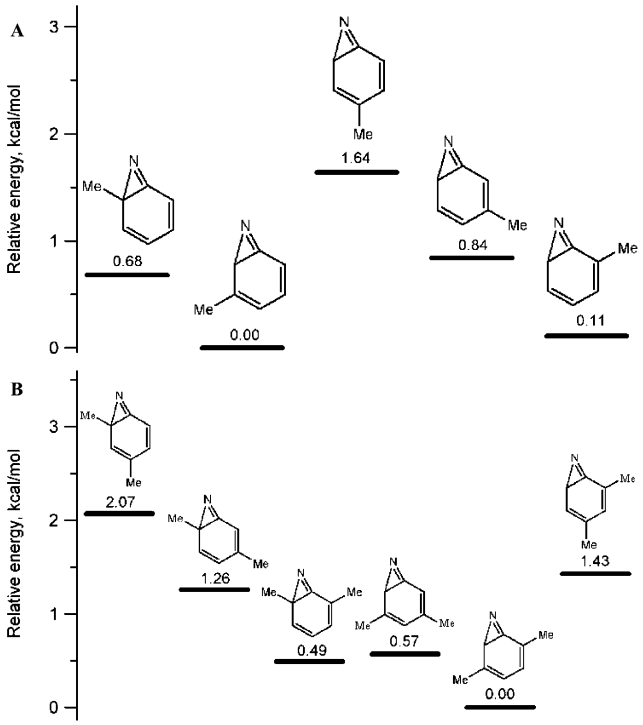

Figure 11. Relative energies of (A) mono- and (B) di- methyl substituted benzazirines using the B3LYP/6-311+G(2d,p)//B3LYP/6-31G* method corrected with the unscaled B3LYP/6-31G* ZPE differences.

Combining this experimental result with the CASPT2 energies, the estimated ΔE_{ST} values for **1b**∼**1f** are 15.6∼16.4 kcal/mol. Note that although the absolute values of ΔE_{ST} computed by the DFT method are about 4 kcal/mol smaller than the CASPT2 energies, the relative energies of ΔE_{ST} predicted by DFT, CASSCF, and CASPT2 are similar.

Ortho alkyl substituents accelerate the rate of intersystem crossing (k_{ISC}) within a factor of 3. The directly observed k_{ISC} of parent phenylnitrene in a rigid glass at 77 K is 3.8×10^6 s^{-1} (Figure S1, Supporting Information), a value very close to the literature value of 3.2×10^6 s^{-1} measured in pentane.[14] The alkyl substituent effects in a glassy matrix can be depicted from the k_{ISC} of **1c**, **1d**, and **1f**, which are 1.0×10^7, 1.2×10^7, and 6.8×10^6 s^{-1}, respectively. This is in agreement with that of the methylated analogues.[22,3d] Furthermore, a small medium effect on k_{ISC} is observed in the case of diethylphenylnitrene. The k_{ISC} rate constant determined from the dynamics of **1c** in solution phase (1.5×10^7 s^{-1}) is slightly faster than that observed in a glassy matrix medium (1.0×10^7 s^{-1}).

The calculated bond lengths in Tables S3−S6 demonstrate that the size of the alkyl substituents have very little influence on the N−C_1 and N−C_2 bond lengths. Calculations predict that the N−C_1 bond lengths of singlet nitrenes **1a**∼**1f** are around 1.274∼1.276 Å, thus their bond orders should be approximately two. This illustrates the biradical character of these singlet nitrenes, which is consistent with published computational results.[14−16] Alkyl substituents have little influence on the C−N

(35) (a) Travers, M. J.; Cowles, D. C.; Clifford, E. P.; Ellison, G. B. *J. Am. Chem. Soc*. **1992**, *114*, 8699. (b) McDonald, R. N.; Davidson, S. J. *J. Am. Chem. Soc*. **1993**, *115*, 10 857.

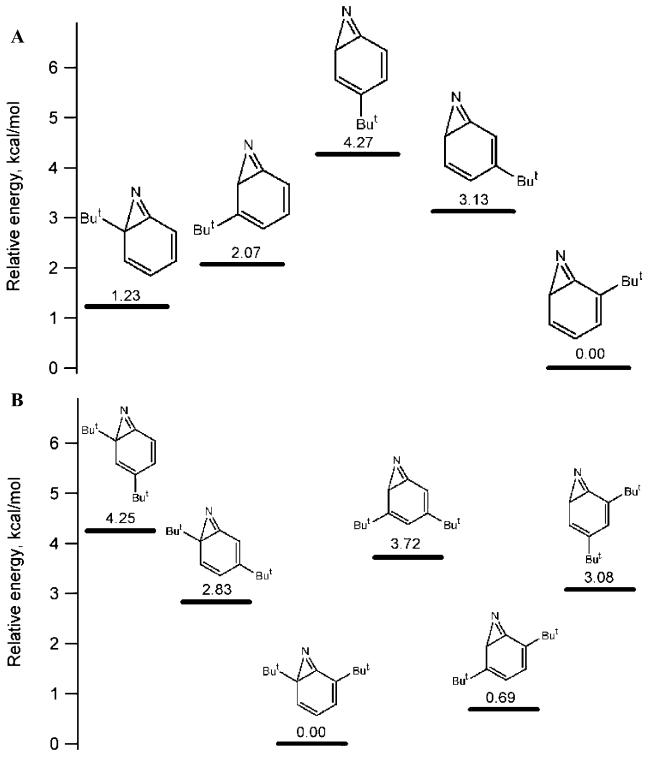

Figure 12. Relative energies of (A) mono- and (B) di- *tert*-butyl substituted benzazirines using the B3LYP/6-311+G(2d,p)//B3LYP/6-31G* method corrected with the unscaled B3LYP/6-31G* ZPE differences.

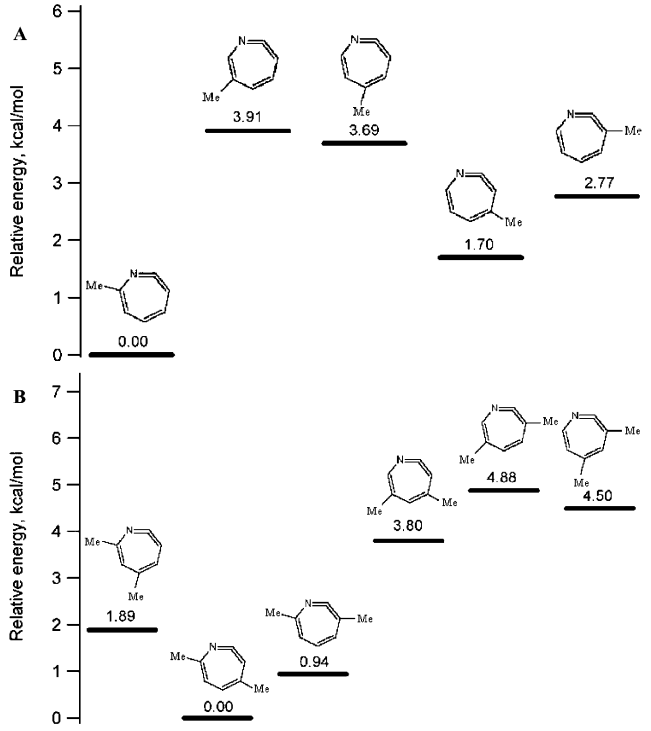

Figure 13. Relative energies of (A) mono- and (B) di- methyl substituted didehydroazepines using the B3LYP/6-311+G(2d,p)//B3LYP/6-31G* method corrected with the unscaled B3LYP/6-31G* ZPE differences.

bond length but not for the C−C bond length, r_2 (Scheme 2, Table S3). It is found that bulkier alkyl groups result in longer values of r_2. This is a result of the higher steric strain present in the singlet nitrene with the larger alkyl substituent. Moreover, d_{N-H}, the distance between the nitrene nitrogen and the closest

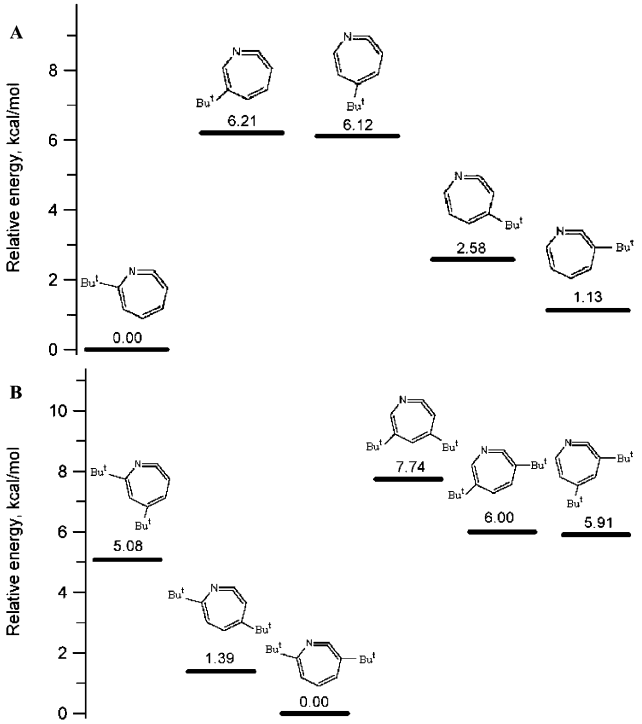

Figure 14. Relative energies of (A) mono- and (B) di- *tert*-butyl substituted didehydroazepines using the B3LYP/6-311+G(2d,p)//B3LYP/6-31G* method corrected with the unscaled B3LYP/6-31G* ZPE differences.

hydrogen of the alkyl substituents is very sensitive to the size of the specific alkyl substituents (Table S7). The value of d_{N-H} becomes shorter going from singlet nitrene **1** to transition state $\mathbf{TS_{1-4}}$ when the alkyl substituents are smaller (substituents **a**, **b**, and **c**) but the distance elongates going from **1** to $\mathbf{TS_{1-4}}$ when the alkyl substituents are bulkier (substituents **d**, **e**, and **f**).

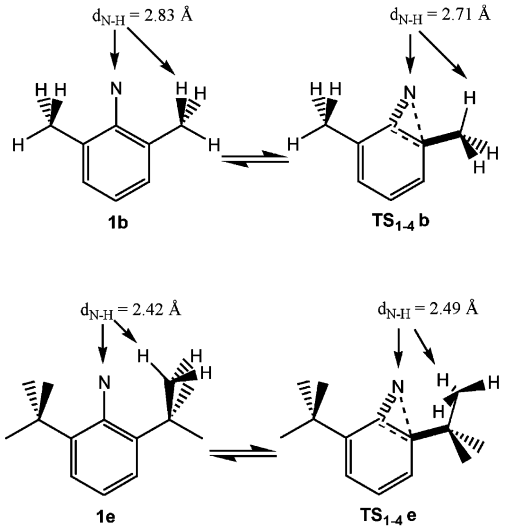

Because d_{N-H} is somewhat related to the steric strain between the nitrogen atom and those alkyl substituents, the changes in d_{N-H} mentioned above indicate that the steric strain is increasing when **1a**, **1b**, and **1c** cyclize but that the steric strain is released during the cyclization of **1d**, **1e**, and **1f**.

E_{a1}, the activation energy of the first cyclization step for singlet phenylnitrenes to rearrangement, is also sensitive to the size of the alkyl substituents. Table S8 and Figure 8 show that

dimethyl and diethyl derivatives have the largest E_{a1} values, but that E_{a1} drops dramatically when the size of alkyl substituents increases with the isopropyl (**1d**) or *tert*-butyl groups (**1e** and **1f**). Inspection of the data in Table S10 and the potential energy surface in Figure 10 reveals that the barrier for 2-*tert*-butylphenylnitrene **1i** to cyclization toward the *tert*-butyl group is only 0.44 kcal/mol greater than that of unsubstituted phenylnitrene **1a** and that the activation energy for **1i** to cyclization away from the *tert*-butyl group is 3.56 kcal/mol lower than that of **1a**. The similar E_{a1} values of **1f** (Figure 8) and of **1i** for the cyclization away from the *tert*-butyl group indicates that the main origin of the dramatic drop of E_{a1} value is due to the strain released between the nitrogen atom and the alkyl substituent that the nitrene nitrogen atom moves away from during the phenylnitrene cyclization process.

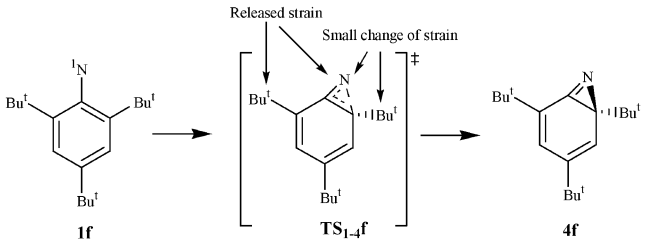

The theoretical finding of alkyl substituent effects on E_{a1} is in excellent agreement with the experimental measurement of the lifetime of singlet phenylnitrenes. The lifetimes of **1a**,[14] **1b**,[22] and **1c** (Figure 2) are determined to be ~1, 12, and 9 ns at ambient temperature, compared to the 6 ns lifetime of **1d** at 260 K (Figure S6). Moreover, the lifetime of **1f** is too short to be measured at ambient temperature.

Theory predicts that the bulkiness of alkyl substituents will alter not only the energy barrier of the first cyclization step, but that of the second ring-expansion step as well. The computational data of Table S9 and Figure 9 indicate that the bulkier alkyl substituents have a greater activation energy for the second step (E_{a2}). Therefore, the more hindered alkyl substituent will lower the barrier of the first step but raise the barrier of the second step. In the extreme case of 2,4,6-tri-*tert*-butyl derivative **1f**, the energy barrier of the second step is larger than that of the first step; that is, unlike **1a**~**1c** whose rate-determining step (RDS) for rearrangement is the cyclization step, **1f** will have the second step, ring-expansion, as its RDS. Inspection of the predicted activation energy in Figures 9 and 10 reveals that the *tert*-butyl substituent on a *para* position raises the E_{a2} energy by 1.43 kcal/mol relative to the parent species, and that a *tert*-butyl substituent at the *ortho* position raises the E_{a2} value by 2.03 kcal/mol for **1i** to rearrangement away from the *tert*-butyl group. As shown in Figure 9, the E_{a2} value of **1f** is 3.33 kcal/mol greater than that of parent phenylnitrene **1a**. This is very close to the combined values (3.46 kcal/mol) of those of **1i** and **1j**, suggesting that the steric effects of both the *ortho* and *para* *tert*-butyl groups play an important role in producing the large E_{a2} energies. Furthermore, a *tert*-butyl substituent at the *para* position also destabilizes the ketenimine intermediate **5j** (Figure 10B). This is consistent with the energy difference between **5e** and **5f** shown in Figure 9.

Because benzazirine **4f** is predicted to be ~5 kcal/mol more stable than **1f** (relative to their corresponding singlet nitrenes) and the rate-determining step for **1f** to rearrangement is the ring-expansion process of **4f** to form ketenimine **5f**, then **4f** is expected be an observable intermediate. Indeed, a transient species with an absorption maximum at 285 nm is observed upon LFP of 2,4,6-tri-*tert*-butylphenyl azide **2f** in pentane at ambient temperature (Figure 5A). This species converts to didehydroazepine **5f** with a time constant of 62 ns at room temperature. The 285 nm transient cannot be attributed to the singlet 2,4,6-tri-*tert*-butylphenyl nitrene **1f** for three reasons. First, it lacks the 363 and 346 nm characteristic absorptions of **1f** observed at 77 K (Figure 1); second, its lifetime at 193 K is significantly longer compared to that of the singlet nitrene at 77 K; and finally, the Arrhenius plot is completely different from that of singlet parent phenylnitrene. The carrier of the 285 nm absorbing transient cannot be attributed to triplet 2,4,6-tri-*tert*-butylphenyl nitrene **3f** as it shows a significant (20 nm) blue shift relative to that of **3f**, observed at 77 K, in a glassy matrix. Furthermore, its 62 ns lifetime in pentane at ambient temperature is too short for a triplet nitrene such as **3f** which is expected to dimerize over hundreds of microseconds to form the azo compound. Thus, the 285 nm transient is attributed to benzazirine **4f**. Time-dependent DFT calculations[36] at the B3LYP/6-31G* level predict that **4f** will absorb strongly at 282 nm, which is in excellent agreement with the experimental result. Also, the calculated activation energy (6.32 kcal/mol, see Table S9) for **4f** to ring expand to form **5f** is very close to the experimental barrier deduced from the temperature dependence of the observed decay rate constants of 285 nm transient absorption (7.4 ± 0.2 kcal/mol).

V. Conclusions

Singlet 2,6-diethylphenylnitrene **1c**, 2,6-diisopropylphenylnitrene **1d**, and 2,4,6-tri-*tert*-butylphenylnitrene **1f** are directly observed in a glassy matrix at 77 K by LFP methods. Alkyl substituents exert a small red shift on the transient absorption of singlet phenylnitrenes. Singlet phenylnitrenes **1c**, **1d**, and **1f** convert to their triplet states exclusively at 77 K with ISC rate constants in the range of $(6.8 \sim 12) \times 10^6$ s^{-1}.

The lifetime of **1c** at ambient temperature in pentane is ~9 ns, which is shorter than that of the 2,6-dimethyl analogue **1b**. The energy barrier for **1c** to rearrangement is determined to be 5.2 ± 0.5 kcal/mol or 6.2~6.7 kcal/mol with compensating changes in the preexponential *A* value, and is smaller than that of **1b**. Furthermore, at 260 K, **1d** has a lifetime of ~6 ns, a value shorter than that of **1c** at ambient temperature.

In the two-step process of the singlet phenylnitrene rearrangement, the energy barrier of the first cyclization step and second ring-expansion step are influenced by the *ortho*,*ortho*-dialkyl substituents. Bulkier alkyl groups lower the barrier of the first step and raise the barrier of the second step, presumably due to the changes in the steric strain in the reactive intermediates and transition states. In the presence of *tert*-butyl substituents at every *ortho* and *para* position, the second step becomes the rate-determining step and benzazirine **4f** becomes observable. LFP of 2,4,6-tri-*tert*-butylphenyl azide in pentane at ambient temperature produces the transient spectrum of **4f**, which absorbs strongly at 285 nm. The lifetime of **4f** is 62 ns in pentane at ambient temperature, and the activation energy

(36) Casida, M. E.; Jamorski, C.; Casida, K. C.; Salahub, D. R. *J. Chem. Phys.* **1998**, *108*, 4439.

for **4f** to ring-expansion to form didehydroazepine **5f** is 7.4 ± 0.2 kcal/mol with a preexponential factor of $10^{12.6\pm0.2}$ s^{-1}.

VI. Experimental Section

Laser Flash Photolysis. Two sets of LFP apparatus were used in this study. In the older version of the spectrometer,[23d] a Nd:YAG laser (Continnum PY62C-10, 266 nm, 150 ps, 10 mJ) or KrF excimer laser (Lumonics, 249 nm, 12 ns, 50 mJ) was used as the excitation light source. The probe light of a pulsed xenon lamp was focused into a 0.25 m grating monochromator (Oriel 77200) and detected with a photomultiplier tube (PMT). The signal from the PMT (Hamamatsu, R928) was recorded with a digitizer (Tektronix 7912AD, 7A29 amplifier, 7B92A time base) and transferred to a personal computer. Transient absorption spectra were recorded using an EG&G Princeton Applied Research model 1460 optical multichannel analyzer (OMA). This instrument was based on a hard-wired computer interface. The new version of the flash photolysis instrument is described elsewhere.[37]

Stock solutions of phenyl azides **2** were prepared in dry spectroscopic grade solvents to an optical density (OD) of about 1.5∼2.0 at the excitation wavelength (266 or 249 nm). The temperature was maintained at 77 K by means of boiling liquid nitrogen or varied in the range of 170 ∼ 300 K by passing a thermo-stabilized nitrogen stream over the sample and kept to within ± 1 K. In these experiments, a quartz cuvette was placed in a quartz cryostat. The sample solutions were changed after every laser shot, unless otherwise indicated.

Time-Resolved Infrared (TRIR) Studies. TRIR experiments were conducted with a JASCO TRIR-1000 dispersive-type IR spectrometer with 16 cm^{-1} resolution following the method described in the literature.[38]

Computational Chemistry. To estimate the singlet−triplet splitting and the energy barrier for singlet phenylnitrenes **1a**∼**1j** to cyclize to form benzazirine **4a**∼**4j**, the geometries of **1a**∼**1j**, their triplet states **3a**∼**3j**, and $\mathbf{TS_{1-4}a}$∼ $\mathbf{TS_{1-4}e}$, the transition state of the cyclization process, were fully optimized using the CASSCF(8,8) method[28] with the 6-31G* (5D) basis set.[29] This (8,8) active space consists of seven π MOs and the in-plane 2p AO on the nitrene nitrogen.[15a] The effects of including dynamic electron correlation are determined by CASPT2/6-31G* calculations[30] for CASSCF(8,8)/6-31G* optimized geometries with CASSCF(8,8)/6-31G* wave functions as a reference. Both CASSCF and CASPT2 calculations are carried out with MOLCAS version 5.0.[39]

To compute the singlet−triplet splitting using the DFT and sum method,[16,33,34] geometries of singlet **1a**∼**1f** and triplet **3a**∼**3f** were fully optimized using the unrestricted B3LYP[31] method with 6-31G* (6D) basis set. For the DFT calculations of **1a**∼**1f** with broken symmetry, their HOMO and LUMO are mixed during the computation so that an $<S^2>$ value of 1.0 is obtained as a 50:50 mixture of their lowest triplet and singlet state. These DFT wave functions were also tested to ensure their stability. Single-point energies were calculated using the UB3LYP/6-311+G(2d,p) method for the UB3LYP/6-31G* optimized geometries. Finally, the DFT singlet−triplet energy gaps were computed from these UB3LYP/6-311+G(2d,p) energies with the sum method (eq 2).[16,33,34]

To explore the reaction path for singlet phenylnitrenes to rearrangement, geometries of proposed reactive intermediates (**4a**∼**4j**, **5a**∼**5j**, **6g**∼**6i**, **7g**∼**7i**) and transition states ($\mathbf{TS_{1-4}a}$∼**j**, $\mathbf{TS_{4-5}a}$∼**j**, $\mathbf{TS_{1-6}g}$∼**i**, $\mathbf{TS_{6-7}g}$∼**i**) were fully optimized by the DFT method at the B3LYP/6-31G* level of theory except $\mathbf{TS_{1-4}a}$∼**j** and $\mathbf{TS_{1-6}g}$∼**i** for which the broken symmetry DFT calculations of UB3LYP/6-31G* were used and yielded the $<S^2>$ values of 0.16∼0.31. Vibrational frequencies were calculated for the (U)B3LYP/6-31G* optimized geometries to analyze the nature of the stationary points (minimum or transition state) and were used to account for ZPE differences. Single-point energies were calculated using the 6-311+G(2d,p) basis set with the same DFT method for the (U)B3LYP/6-31G* optimized geometries. Time dependent DFT calculations[36] of **3a**∼**f**, **4a**∼**f**, and **5a**∼**f** were performed at the B3LYP/6-31G* level of theory.

To investigate the alkyl substituent effects on the stability of benzazirine **4** and didehydroazepine **5**, the geometries of a series of monomethyl, dimethyl, mono-*tert*-butyl, and di-*tert*-butyl substituted benzazirines and didehydroazepines (see Figures 15−18 for structures) were optimized using the B3LYP/6-31G* method. The relative energies of these species were then computed using the B3LYP/6-311+G(2d,p)//B3LYP/6-31G* method and were corrected with the B3LYP/6-31G* ZPE differences.

All DFT calculations were carried out with GAUSSIAN 98.[40]

Materials. Pentane, hexane, and acetonitrile (Aldrich) are spectroscopic grade and used as received. Diethyl ether and *n*-BuLi hexane solution were used as received. THF was refluxed over sodium and distilled under argon prior to use. Commercially available 2,6-diethylaniline, 2,6-diisopropylaniline, and 2,4,6-tri-*tert*-butyl aniline (Aldrich) were used without further purification. The preparation of 2,6-diethylphenyl azide,[41] 2,6-diisopropylphenyl azide,[41] and 2,4,6-tri-*tert*-butylphenyl azide[42] followed the procedures described in the literature.

Acknowledgment. Support of this work by the National Science Foundation and the Ohio Supercomputer Center is gratefully acknowledged. One of us (M.L.T.) thanks the Ohio State University for a Presidential Fellowship.

Supporting Information Available: The transient UV−visible spectra produced upon LFP of **2a**, **2c**, and **2d** in 3-methylpentane at 77 K and **2c**, **2d**, and **2f** in pentane at 193 K. The temperature dependence of the observed rate constants for the decay of **1c** and **4f** in pentane. The selected bond-distances in **1a**∼**1f** and **3a**∼**3f**, and in structures **1**, $\mathbf{TS_{1-4}}$, **4**, $\mathbf{TS_{4-5}}$, and **5** of Scheme 3. Computational data including Cartesian coordinates of all optimized geometries, electronic and zero-point vibrational energies, and TD-DFT absorption maxima and oscillator strengths. This material is available free of charge via the Internet at http://pubs.acs.org.

JA035833E

(37) Martin, C. B.; Shi, X.; Tsao, M.-L.; Karweik, D.; Brooke, J.; Hadad, C. M.; Platz, M. S. *J. Phys. Chem. B* **2002**, *106*, 10 263.
(38) (a) Yuzawa, T.; Kato, C.; George, M. W.; Hamaguchi, H. *Appl. Spectrosc.* **1994**, *48*, 684. (b) Iwata, K.; Hamaguchi, H. *Appl. Spectrosc.* **1990**, *44*, 1431. (c) Toscano, J. P. *Adv. Photochem.* **2001**, *26*, 41.
(39) MOLCAS Version 5. Andersson, K.; Barysz, M.; Bernhardsson, A.; Blomberg, M. R. A.; Cooper, D. L.; Fleig, T.; Fülscher, M. P.; de Graaf, C.; Hess, B. A.; Karlström, G.; Lindh, R.; Malmqvist, P.-Å.; Neogrády, P.; Olsen, J.; Roos, B. O.; Sadlej, A. J.; Schütz, M.; Schimmelpfennig, B.; Seijo, L.; Serrano-Andrés, L.; Siegbahn, P. E. M.; Stålring, J.; Thorsteinsson, T.; Veryazov, V.; Widmark, P.-O. Lund University, Sweden, 2000.
(40) Frisch, M. J.; Trucks, G. W.; Schlegel, H. B.; Scuseria, G. E.; Robb, M. A.; Cheeseman, J. R.; Zakrzewski, V. G.; Montgomery, J. A., Jr.; Stratmann, R. E.; Burant, J. C.; Dapprich, S.; Millam, J. M.; Daniels, A. D.; Kudin, K. N.; Strain, M. C.; Farkas, O.; Tomasi, J.; Barone, V.; Cossi, M.; Cammi, R.; Mennucci, B.; Pomelli, C.; Adamo, C.; Clifford, S.; Ochterski, J.; Petersson, G. A.; Ayala, P. Y.; Cui, Q.; Morokuma, K.; Malick, D. K.; Rabuck, A. D.; Raghavachari, K.; Foresman, J. B.; Cioslowski, J.; Ortiz, J. V.; Stefanov, B. B.; Liu, G.; Liashenko, A.; Piskorz, P.; Komaromi, I.; Gomperts, R.; Martin, R. L.; Fox, D. J.; Keith, T.; Al-Laham, M. A.; Peng, C. Y.; Nanayakkara, A.; Gonzalez, C.; Challacombe, M.; Gill, P. M. W.; Johnson, B. G.; Chen, W.; Wong, M. W.; Andres, J. L.; Head-Gordon, M.; Replogle, E. S.; Pople, J. A. *Gaussian 98*, revision A.9; Gaussian, Inc.: Pittsburgh, PA, 1998.
(41) Murata, S.; Abe, S.; Tomioka, H. *J. Org. Chem.* **1997**, *62*, 3055.
(42) (a) Anselme, J.-P.; Fisher, W. *Tetrahedron*, **1969**, *25*, 855. (b) Nakajima, M.; Anselme, J.-P. *Tetrahedron Lett.* **1976**, *49*, 4421.